A Novel Strategy for Programmable DNA Tile Self-Assembly with DNAzyme-Mediated DNA Cross Circuit

(Supplementary Information)

Siqi Gao, †[a] Ranfeng Wu †[b] and Qiang Zhang *[a, b]

a Key Laboratory of Advanced Design and Intelligent Computing, Dalian University, Ministry of Education, Dalian 116622, China. Email: Gaosiqi1997@163.com

b School of Computer Science and Technology, Dalian University of Technology, Dalian 116024, China. Email: zhangq@dlut.edu.cn

† These authors contributed equally to this work.

Contents

S1. Feasibility of cross circuit

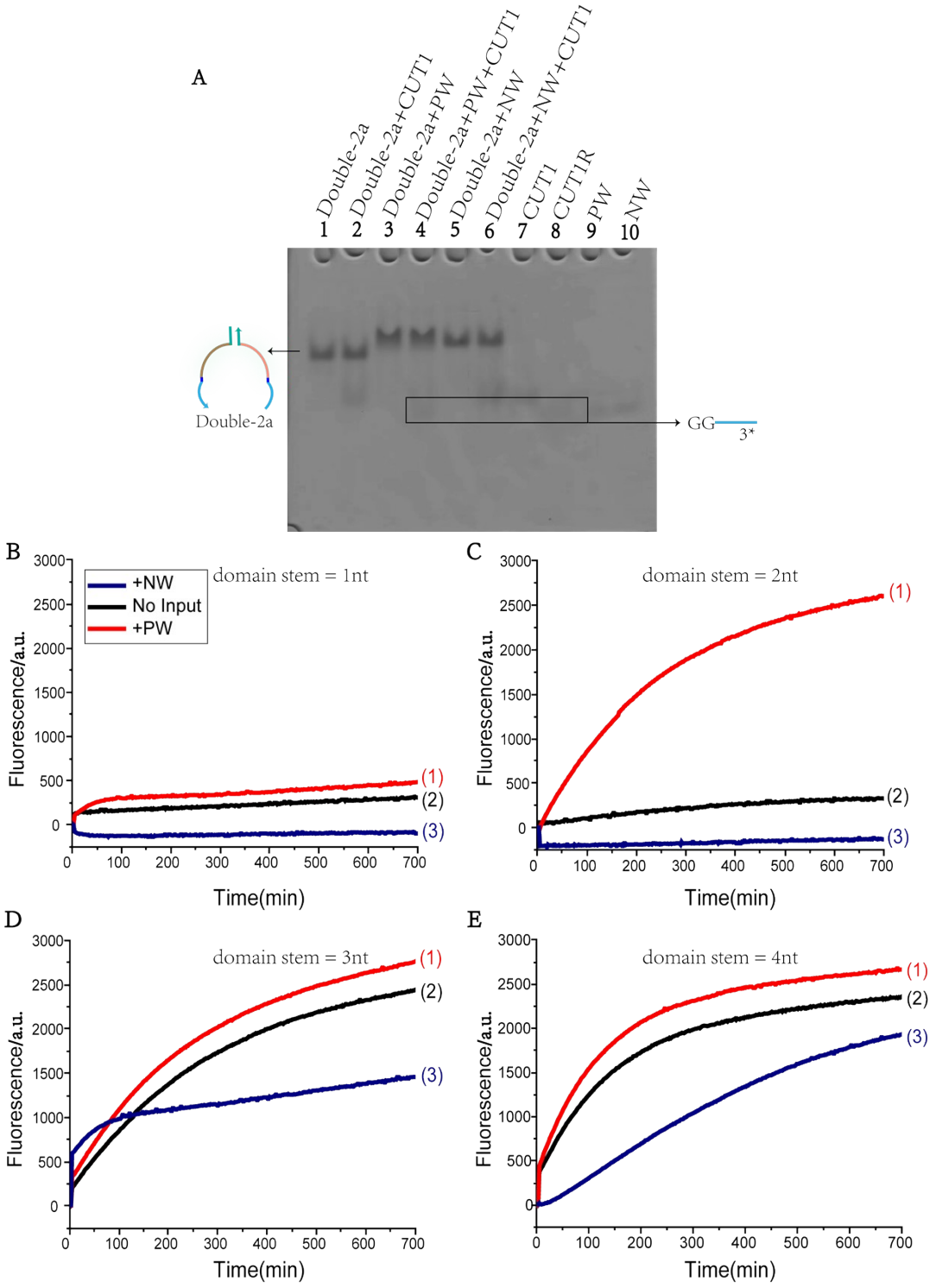

Fig. S1. Feasibility of cross circuit. (A) Native PAGE analysis of the feasibility of cross circuit. The DNA strands involved are labeled above the PAGE. ([Double-2a]: [PW]: [CUT1] = 1: 1: 1, [Double-2a]: [NW]: [CUT1] = 1: 1: 1, [CUT1] = 0.4 μM). (B), (C), (D) and (E) Analysis of the fluorescence kinetics of the number of bases pairing of the domain stem and stem*.

We verified the feasibility of the bidirectional control of DNAzyme activity

strategy by analyzing the results of polyacrylamide gel electrophoresis (PAGE) experiment, as shown in Fig. S1A. The band in lane 8 represents the strand CUT1R, which is used to compare the output of different inputs. Lanes 2, 4, and 6 represent the reaction when there is no input and the input is PW and NW. In lanes 2 and 6, there is no new band corresponding to CUT1R, which proves that the CUT1 has not been cleaved. In lane 4, a new band corresponding to CUT1R is produced, which proves that when PW is input, the complex Double-2a/PW (lane 3) is formed and the CUT1 is cleaved. Note that after the DNAzyme cuts CUT1, two single strands are generated, including CUT1R, but the sequence is too short to be displayed on the PAGE, so the base T is added to extend the sequence without affecting the experimental results.

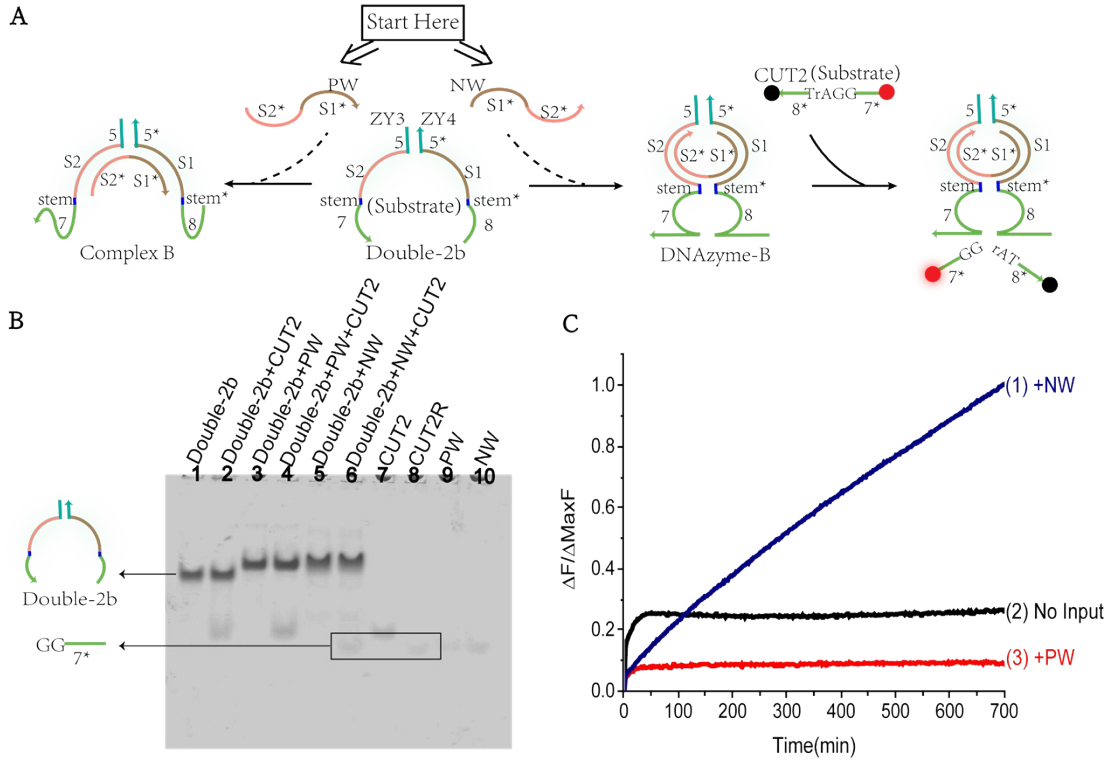

Fig. S2. (A) Schematic diagram of bidirectional control of DNAzyme activity. (B) Native PAGE analysis of the feasibility of cross circuit. The DNA strands involved are labeled above the PAGE. ([Double-2b]: [PW]: [CUT2] = 1: 1: 1, [Double-2b]: [NW]: [CUT2] = 1: 1: 1, [CUT2] = 0.4 μM). (C) Analysis of fluorescence kinetics of feasibility of the cross circuit. Each curve represents inputs with Double-2b and CUT2 as substrates, and the inputs have been marked in the figure. ([Double-2b]: [PW]: [CUT2] = 1: 1: 1, [Double-2b]: [NW]: [CUT2] = 1: 1: 1, [CUT2] = 0.2 μM).

To further demonstrate the success of the bidirectional control of DNAzyme activity strategy, it was further tested on additional DNA sequences. Therefore, two other single strands ZY3 and ZY4 are designed to form double-2b. We conducted polyacrylamide gel electrophoresis experiments and real-time PCR experiments. As shown in Fig. S2B. The band in lane 8 represents the strand CUT2R, which is used to compare the output of different inputs. Lanes 2, 4, and 6 represent the reaction when there is no input and the input is PW and NW. In lanes 2 and 4, there is no new band corresponding to CUT2R, which proves that the CUT2 has not been cleaved. In lane 6, a new band corresponding to CUT2R is produced, which proves that when PW is

input, the complex Double-2b/NW (lane 5) is formed and the CUT2 is cleaved. At the same time, we performed fluorescence kinetic analysis, as shown in Fig. S2C. In the presence of the input strand NW (curve 1), there is a fluorescence rise signal. The experimental results prove the success of the bidirectional control of DNAzyme activity strategy.

S2. The influence factor of cross circuit

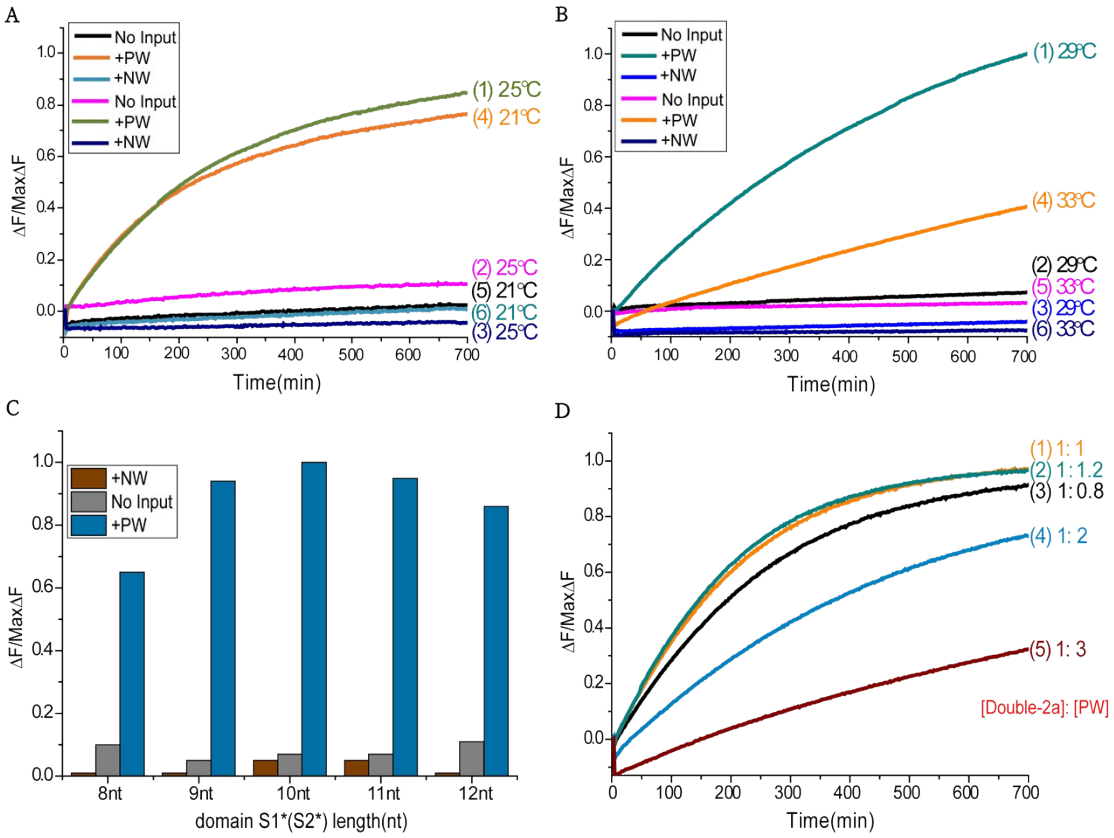

Fig. S3. The influence factors of cross circuit. (A) Fluorescence kinetic analysis at 21°C and 25°C. (B) Fluorescence kinetic analysis at 29°C and 33°C. Each curve represents inputs with Dou-ble-2a and CUT1 as substrates, and the inputs have been marked in the figure. ([Double-2a]: [PW]: [CUT1] = 1: 1: 1, [Double-2a]: [NW]: [CUT1] = 1: 1: 1, [CUT1] = 0.2 μM). (C) Statis-tical analysis of input strands (PW and NW) of different lengths, i.e., the number of bases of the domain S1*(and domain S2*) in the input strands is 8 nt-12 nt. Each group of the histogram represents the inputs with Double-2a and CUT1 as substrates, and the inputs have been marked in the figure. ([Double-2a]: [PW]: [CUT1] = 1: 1: 1, [Double-2a]: [NW]: [CUT1] = 1: 1: 1, [CUT1] = 0.2 μM). (D) Fluorescence kinetic analysis of different ratios of Double-2a to PW concentration. The concentration ratio of Double-2a to PW is represent-ed by each curve. Except for the different concentration ratios, all other reaction conditions are the same. The reaction substrates are Double-2a and CUT1. ([Double-2a] = [CUT1] = 0.2 μM).

To verify whether the hybridization between the input strands (PW and NW) and the double-stranded Double-2a is affected by temperature, we changed the temperature while leaving the other conditions unchanged and performed fluorescence kinetic analysis (Fig. S3A and Fig. S3B). As shown in Fig. S3A, curves (1) and (4) respectively reflect the increase in fluorescence intensity when the input

strand PW is added at 25°C and 21°C. Experimental results show that the cutting rate of DNAzymes is almost the same, and cooling has little effect on the system. As shown in Fig. S3B, when the input strand PW is added, the curve (1) fluorescence signal rises and the curve (4) fluorescence signal does not increase significantly. The experimental results show that as the temperature rises, the cut-ting rate of DNAzymes decreases accordingly, so the high temperature system environment is not selected. Therefore, the reaction temperature at 25°C is finally selected.

Through real-time PCR experiments, we explored the influence of input strands of different lengths on DNAzyme activity. Statistical analysis of this is shown in Fig. S3C, and the brown histogram and gray histogram respectively represent the fluorescence intensity with input NW and no input, and a relatively lower fluorescence intensity is observed. Therefore, by comparing with the fluores-cence intensity of the input PW represented by the blue histogram, the optimal input strand length is obtained. When the length of domain S1* (and domain S2*) is 10 nt, the activity of DNAzyme is highest, so the length of the optimal input strand is 20 nt.

Next, by controlling the concentration of PW, we observed the fluorescence intensity change. As shown in Fig. S3D, the fluorescence curve rises to varying degrees. With the increase of the con-centration, the rise of the fluorescence curve keeps increasing. When [Double-2a]: [PW] = 1: 1, the DNAzyme cleavage rate is the largest. As the PW concentration exceeds a fixed amount of CUT1, the rise of the fluorescence curve shows a decreasing trend. As the concentration of PW increases, the promotion effect gradually decreases. This is because at the beginning of the reaction, there are multiple forms of Double-2a and PW in the solution. However, only when one Double-2a may bind to one PW will the DNAzyme-A cleavage reaction occur. And in this case, the binding of PW to Double-2a is the most stable.[1] Therefore, when PW concentration exceeds a certain range, the binding of one Double-2a to one PW will be reduced, resulting in decreased promotion effect of PW.

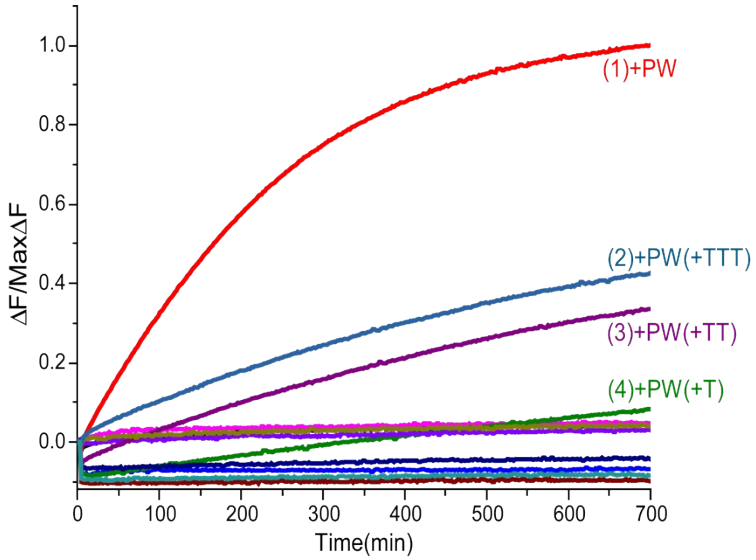

Fig. S4. Analysis of the fluorescence kinetics of adding spacer base T to the input strand. Each curve represents inputs with Double-2a and CUT1 as substrates, and the inputs have been marked in the figure. ([Double-2a]: [PW]: [CUT1] = 1: 1: 1, [Double-2a]: [NW]: [CUT1] = 1: 1: 1, [CUT1] = 0.2 μM).

Considering that the input strand affects the stability of stem and stem* connections, and thus affect the activity of DNAzyme. The number of base T added at the junction of S1* and S2* sequences of the input chain domain is explored. Experimental results prove that adding T base at the junction of domain S1* and S2* sequence will reduce DNAzyme activity.

S3. Analysis of the results of the cross circuit

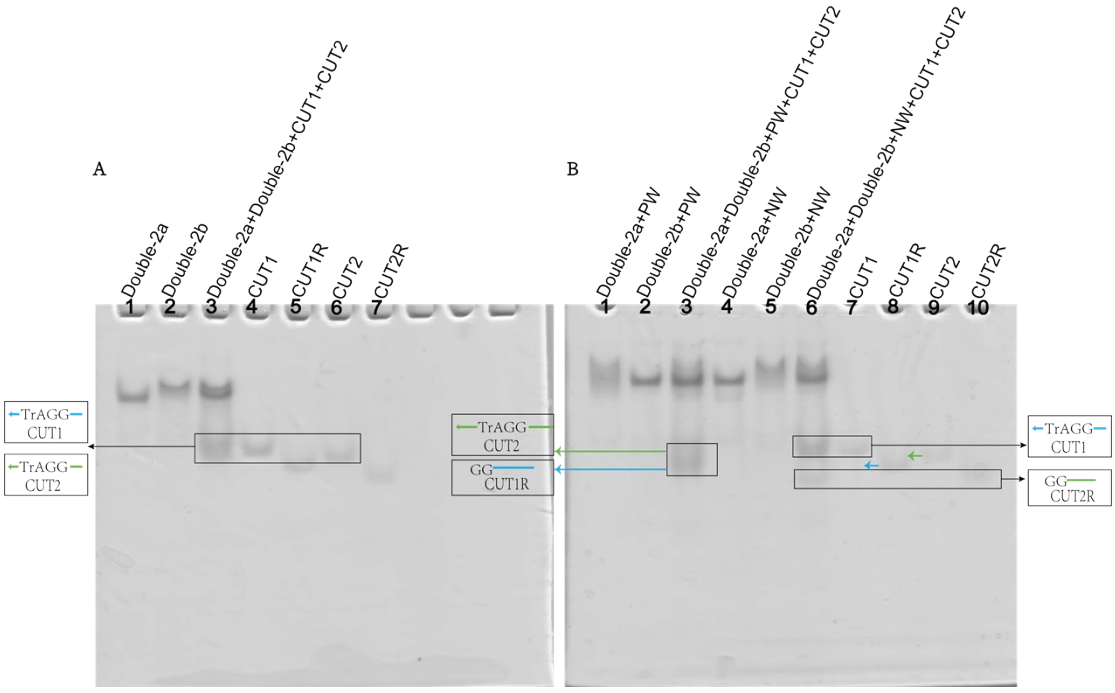

Fig. S5. Analysis of the results of the cross circuit. Native PAGE analysis of the cross circuit. The DNA strands involved are labeled above the PAGE. ([Double-2a]: [Double-2b]: [PW]: [CUT1]: [CUT2] = 1: 1: 2: 1: 1, [Double-2a]: [Double-2b]: [NW]: [CUT1]: [CUT2] = 1: 1: 2: 1: 1, [CUT2] = 0.4 μM).

We verified the feasibility of the bidirectional control of DNAzyme activity strategy by analyzing the results of polyacrylamide gel electrophoresis (PAGE) experiment, as shown in Fig. S5. When there is no input, lane 3 is shown in Fig. S5A, the two double-stranded structures (Double-2a and Double-2b) and the two single strands (CUT1 and CUT2) initially coexist in the solution and do not react. When the input strand PW is added, lane 3 is shown in Fig. S5B, Double-2a/PW recognizes the specific cleavage site (TrAGG) in CUT1 for cleavage, a new band corresponding to CUT1R is produced. PW hybridizes with Double-2b to form Double-2b/PW, which inhibits the cleavage of the substrate CUT2. Similarly, when the input strand NW is added, lane 6 is shown in Fig. S5B, Double-2a/PW inhibits the cleavage of the substrate CUT1, and Double-2b/NW recognizes CUT2 for cleavage, a new band corresponding to CUT2R is produced. Different inputs are completed to control

different DNAzymes for cleavage, and a programmable cross circuit is realized.

S4. Tile protection mechanism

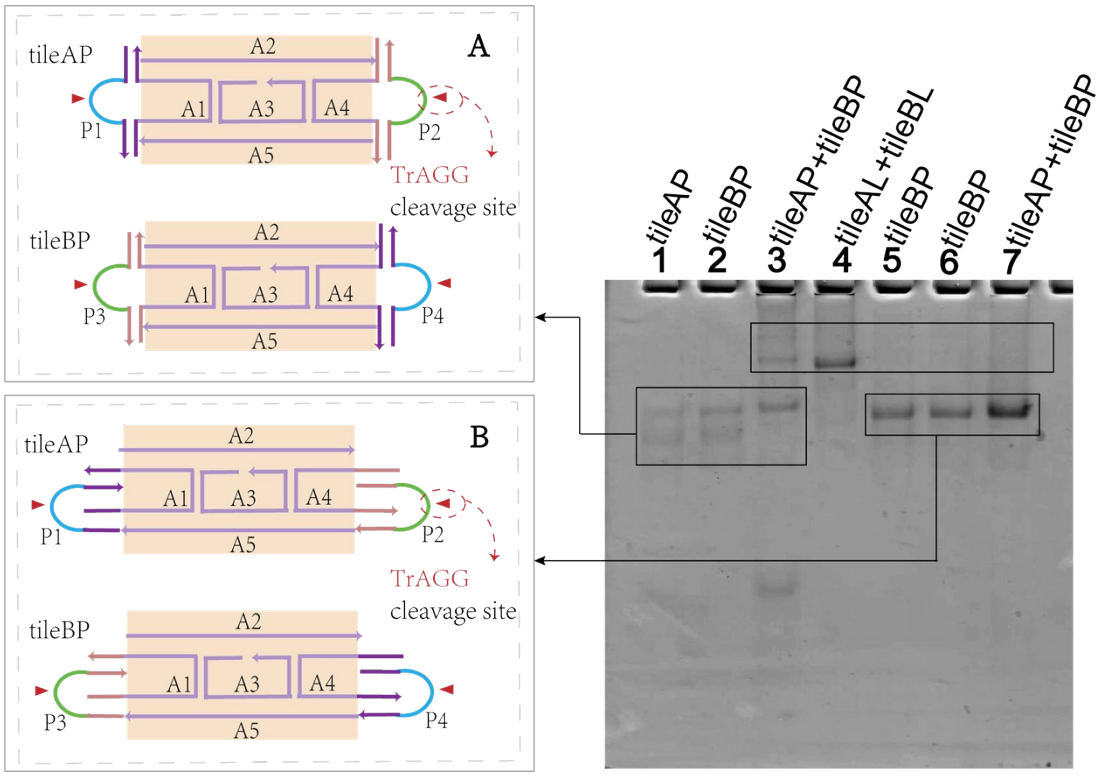

Fig. S6. Tile protection mechanism. Native PAGE analysis of tile protection mechanism. The DNA strands involved are labeled above the PAGE. ([tileAP] = [tileBP] =[tileAL] = [tileBL] = 0.1 μM).

On the basis of DAE tiles, the protection mechanism with DNA cleavage sites is introduced into the self-assembly of tiles to enrich the diversity of tile self-assembly methods. This strategy of combining DNAzymes with protection mechanisms not only satisfies that the cleavage site in the protection mechanism can be specifically recognized and cleaved by DNAzymes, but also uses the double-stranded part of the protection mechanism to pre-protect DNA strands (sticky end) participating in downstream reactions. To control tile self-assembly, two protection mechanisms are illustrated in Fig. S6. The tile and the protection strand are pre-hybridized to become a component of the reaction tile. In order for the controlling tile self-assembly to operate normally, the following conditions must be met: (1) When no input is added, tileAP, tileBP, Double-2a and Double-2b coexist in the solution without reaction. (2) When the input strand PW is added, DNAzyme-A is activated to cut the protection strands P1 and P4. After adding the input strand NW, DNAzyme-B is activated to cleave the protection strands P2 and P3. (3) The structure of the sticky end and the protection strand needs to be specially designed. It is necessary to ensure that the downstream reaction does not occur without input and that the protection domain can be separated from the sticky end automatically after cleavage. Therefore, the

connection method between the sticky end and the protection strand plays a major role in the optimization of the system.

Then we performed polyacrylamide gel electrophoresis (PAGE) experiment to verify the stability of the two protection mechanisms. Lanes 1, 2 and 3 represent tile protection mechanism A, Lanes 4, 5, 6 and 7 represent tile protection mechanism B, As can be seen from lanes 1 and 2, the tile structure formed by the protection mechanism A is unstable. And lane 3 shows protection mechanism A, there is leakage when two tiles coexist. Experiments show that protection mechanism B is better than protection mechanism A.

S5. Feasibility of cross circuit control tile self-assembly

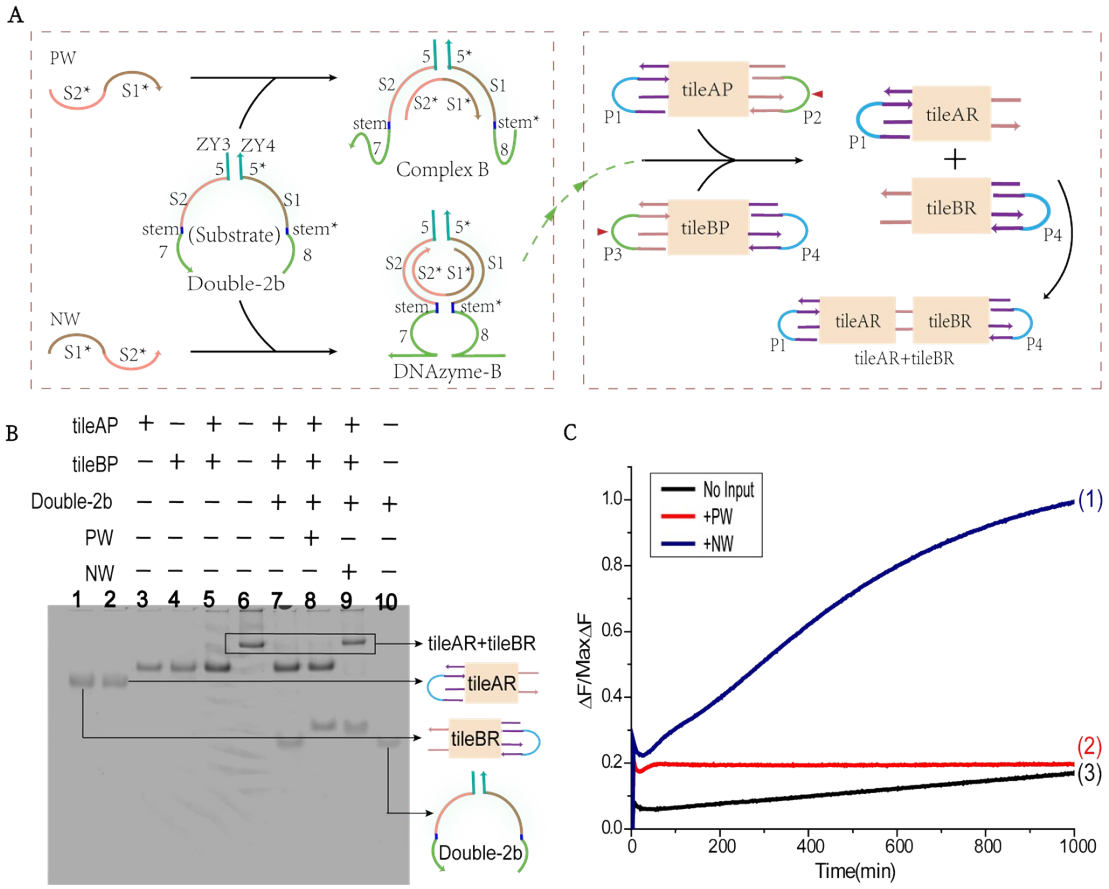

Fig. S7 (A) Schematic diagram of bidirectional regulation of DNAzyme activity strategy to control tile self-assembly. (B) Native PAGE analysis of the feasibility of cross circuit control tile self-assembly. The DNA strands involved are labeled above the PAGE. ([Double-2b]: [PW]: [tileAP]: [tileBP] = 2: 2: 1: 1, [Double-2b]: [NW]: [tileAP]: [tileBP] = 2: 2: 1: 1, [tileAP] = 0.1 μM). (C) Analysis of fluorescence kinetics of feasibility of cross circuit control tile self-assembly. Each curve represents inputs with Double-2b, tileAP and tileBP as substrates, and the inputs have been marked in the figure. ([Double-2b]: [PW]: [tileAP]: [tileBP] = 2: 2: 1: 1, [Double-2b]: [NW]: [tileAP]: [tileBP] = 2: 2: 1: 1, [tileAP] = 0.1 μM).

As shown in Fig. S7A, once the trigger strand NW is input, the DNAzyme-B signal

molecule is generated to cut the protection strands P2 and P3 of the tiles, thereby promoting the self-assemble of the tiles. Under the action of the input strand, the self-assembly of tiles is controlled. In order to verify the feasibility of this mechanism, we conducted polyacrylamide gel electrophoresis experiments and real-time PCR experiments. Fig. S7B shows the experimental results of polyacrylamide gel electrophoresis. The band in lane 6 represents the output strand tileAR + tileBR, which is used to compare the response of different inputs. Lanes 7, 8, and 9 represent the reaction when there is no input and the input strand is PW and NW. In lanes 7 and 8, there is no new band corresponding to tileAR + tileBR, which proves that the tile protection domain is not cut. In lane 9, a new band corresponding to tileAR + tileBR is generated, which proves that when the input strand NW is added, the complex Double-2b/NW is formed, and the tile protection domain is automatically separated from the sticky end of the tile after being cleaved. Sticky end connection. Only when NW and Double-2b coexist, will the two tiles be connected. The fluorescence results are shown in Fig. S7C. When there is no input (curve 3) and when the input is PW (curve 2), there is no change in the fluorescence signal. When the NW is input (curve 1), the complex Double-2b/NW will cut the protection domains P2 and P3, P2 and P3 are automatically separated from the sticky end of the tile. The two tiles are connected through the exposed sticky ends, the fluorophore is separated from the quencher, and the fluorescent signal increases. polyacrylamide gel electrophoresis experiments and real-time PCR experiments prove the feasibility of programmable control tile self-assembly.

S6. DNA sequence

Table S1. DNA sequences and modifications

Strand	Sequence (5′ to 3′)	Length(nt)
ZY1	TGACATCAGCGATGAACCCCTATTCCTACCAC CAAATACCCAC	43
ZY2	GTGGGTATTTGGTGGTAGCCTTTTGCTATCCA CCCATGTTACTCTG	46
PW	GAATAGGGGTTAGCAAAAGG	20
NW	TAGCAAAAGGGAATAGGGGT	20
CUT1	FAM-CAGAGTATrAGGATGTCA-BHQ1	17
ZY1(stem-1)	TGACATCAGCGATGACCCCTATTCCTACCACC AAATACCCAC	42
ZY2(stem*-1)	GTGGGTATTTGGTGGTAGCCTTTTGCTACCAC CCATGTTACTCTG	45
ZY1(stem-3)	TGACATCAGCGATCATACCCCTATTCCTACCA CCAAATACCCAC	44
ZY2(stem*-3)	GTGGGTATTTGGTGGTAGCCTTTTGCTAATGC ACCCATGTTACTCTG	47
ZY1(stem-4)	TGACATCAGCGATAGTGACCCCTATTCCTACC ACCAAATACCCAC	45
ZY2(stem*-4)	GTGGGTATTTGGTGGTAGCCTTTTGCTACACT CACCCATGTTACTCTG	48
ZY1(S1-8)	TGACATCAGCGATGAACCCATTCCTACCACCA AATACCCAC	41

ZY2(S2-8)	GTGGGTATTTGGTGGTAGCCTTTCTATCCACC CATGTTACTCTG	44
ZY1(S1-9)	TGACATCAGCGATGAACCCCATTCCTACCACC AAATACCCAC	42
ZY2(S2-9)	GTGGGTATTTGGTGGTAGCCTTTTCTATCCAC CCATGTTACTCTG	45
ZY1(S1-11)	TGACATCAGCGATGAACCCCTAGTTCCTACCA CCAAATACCCAC	44
ZY2(S2-11)	GTGGGTATTTGGTGGTAGCCTTGTTGCTATCC ACCCATGTTACTCTG	47
ZY1(S1-12)	TGACATCAGCGATGAACCACCTAGTTCCTACC ACCAAATACCCAC	45
ZY2(S2-12)	GTGGGTATTTGGTGGTAGCCTTGTATGCTATC CACCCATGTTACTCTG	48
PW (S1*-8, S2*-8)	GAATGGGTTAGAAAGG	16
NW (S1*-8, S2*-8)	TAGAAAGGGAATGGGT	16
PW (S1*-9, S2*-9)	GAATGGGGTTAGAAAAGG	18
NW (S1*-9, S2*-9)	TAGAAAAGGGAATGGGGT	18
PW (S1*-11, S2*-11)	GAACTAGGGGTTAGCAACAAGG	22
NW (S1*-11, S2*-11)	TAGCAACAAGGGAACTAGGGGT	22
PW (S1*-12, S2*-12)	GAACTAGGTGGTTAGCATACAAGG	24
NW (S1*-12, S2*-12)	TAGCATACAAGGGAACTAGGTGGT	24
PW (+T)	GAATAGGGGTTTAGCAAAAGG	21
NW (+T)	TAGCAAAAGGTGAATAGGGGT	21
PW (+TT)	GAATAGGGGTTTTAGCAAAAGG	22
NW (+TT)	TAGCAAAAGGTTGAATAGGGGT	22
PW (+TTT)	GAATAGGGGTTTTTAGCAAAAGG	23
NW (+TTT)	TAGCAAAAGGTTTGAATAGGGGT	23
ZY3	ACTGCTCAGCGATGACCTTTTGCTACTACCAC CAAATACCCAC	43
ZY4	GTGGGTATTTGGTGGTAGACCCCTATTCTCCA CCCATGTTACACT	45
CUT2	ROX-CAGTGTATrAGGAGCAGT-BHQ2	17
A1	CACAGAGGAACGATGAACCCTGGAGCACACC TCTCA	36
A2 (tileBP)	GCTCCAGGCGGTATCCGACCCTGTGGCGTTGG ACCAT-BHQ1	37
A2 (tileAP)	GCTCCAGGCGGTATCCGACCCTGTGGCGTTGG ACCAT-BHQ2	37
A3	GTCGGATACCGCTGGCTTGCCTAGAGTCACCA ACGCCACAGG	42
A4	TCGTCACTCAATGGTCCACTAATCCTCTAAGT GCGT	36
A5	AGGATTAGTGGTGACTCTAGGCAAGCCAGGT TCATCG	37
B1	TGAGTGACGACGATGAACCCTGGAGCACGCA CTTAG	36
B4	TTCCTCTGTGATGGTCCACTAATCCTTGAGAG GTGT	36
P1 (Fig. 6A)	TGAGAGGTGTTTTTTTCAGAGTATrAGGATGTC ATTTTTTTTCCTCTGTG	49
P2 (Fig. 6A)	ROX-ACGCACTTAGTTTTTTCAGTGTATrAGGAGCA GTTTTTTTTGAGTGACGA	49
P3 (Fig. 6A)	CTAAGTGCGTTTTTTTCAGTGTATrAGGAGCAG TTTTTTTTCGTCACTCA	49
P4 (Fig. 6A)	FAM-	49

	ACACCTCTCATTTTTTCAGAGTATrAGGATGTC ATTTTTTCACAGAGGAA	
P1 (Fig. 6B)	TTCCTCTGTGTTTTTTTGCATAGTrAGGCTTGT GTTTTTTTGAGAGGTGT	49
P2 (Fig. 6B)	TGAGTGACGATTTTTTAGAAGAGTrAGGAACG TGTTTTTTACGCACTTAG	49
P3 (Fig. 6B)	TCGTCACTCATTTTTTAGAAGAGTrAGGAACG TGTTTTTTCTAAGTGCGT	49
P4 (Fig. 6B)	CACAGAGGAATTTTTTTGCATAGTrAGGCTTGT GTTTTTTACACCTCTCA	49

1 L. Q. Liu, Q. Y. Hu, W. K. Zhang, W. H. Li, W. Zhang, Z. H. Ming, L. J. Li, N. Chen, H. B. Wang and X. J. Xiao, *Acs Nano*, 2021, **15**, 11573-11584.